High-speed, high-sensitivity aerosol fluorescence spectrum detection using a 32-anode photomultiplier tube detector

Yong-le Pan
Physical Sciences Laboratory, New Mexico State University, Las Cruces, New Mexico 88003-8002

Patrick Cobler and Scott Rhodes
Vtech Engineering Corporation, 20 New England Business Center, Andover, Massachusetts 01810-1077

Alexander Potter, Tim Chou, Stephen Holler, and Richard K. Chang[a)]
Department of Applied Physics and Center for Laser Diagnostics, Yale University, New Haven, Connecticut 06520-8284

Ronald G. Pinnick
U.S. Army Research Laboratory, Computational and Information Sciences Directorate, Adelphi, Maryland 20783-1197

Jean-Pierre Wolf
LASIM (UMR CNRS 5579), Universite Claude Bernard Lyon 1 43, Blvd. du 11 Novembre 1918, 69622 Villeurbanne, France

(Received 3 October 2000; accepted for publication 4 December 2000)

We employ a 32-anode photomultiplier tube (PMT) in a fluorescence detection system and demonstrate its ability to record broad fluorescence spectra at frame rates in excess of 1.4×10^3 Hz, which is 56× faster than the frame rate of an intensified charge coupled device detector. The multi-anode PMT has single-photon detectable sensitivity. A new data acquisition and processing system for the multi-anode PMT, together with the system-controlling software, has been developed. The performance characteristics of the fluorescence detection system, including the data rate capability, dynamic range, signal-to-noise ratio, and crosstalk among the different anodes, are reported. The 32-anode PMT and acquisition system are suitable for a real-time, field-portable, multichannel optical analyzer. © *2001 American Institute of Physics.* [DOI: 10.1063/1.1344179]

I. INTRODUCTION

Techniques for the *in situ*, real-time detection of aerosols, particularly biological aerosols, have significantly advanced during the last several years. These advances have been driven by the concern that airborne microorganisms can cause disease and respiratory problems in hazardous work environments. In addition, some are feared as possible biowarfare agents. Methods that exploit the intrinsic fluorescence of biological molecules found in biological particles as a diagnostic for their detection are beginning to mature. These methods have been used to distinguish bio-aerosols from nonbiological aerosols and to partially classify biological particles.[1–9] Fluorescence-based sensors may provide a rapid diagnostic tool for bio-aerosol classification.[1,2,4,5,8]

A photomultiplier tube (PMT) is one of the most sensitive detectors. It has fast response time (~1 ns), needs no water cooling, and is compact. PMTs have been used to detect the intensity of the elastic scattering and fluorescence in several wavelength bands.[1,3,6,7] The intensified charge coupled device (ICCD) camera has much higher spatial resolution. Both detectors have single-photon sensitivity, however the ICCD generally needs cooling to yield this level of sensitivity. The ICCD camera has been employed for measuring fluorescence spectra from single micrometer-sized particles.[2,4,8] The multi-pixel high gain avalanche photodiode[9] and intensified linear photodiode array[5] have also been used for the detection of elastic scattering patterns and fluorescence spectra. The avalanche photodiode and CCD camera have less gain and lower sensitivity compared to the PMT.

Recent advances have demonstrated the ability to detect UV-excited single-shot fluorescence spectra from single aggregates of *Bacillus subtilis* spores as small as 1.8 μm diameter using an ICCD.[8] However, the slow data-transfer rate of the ICCD detector limits the overall recording speed to 25 spectra per second. A more capable real-time fluorescence detection system needs higher sampling rates in order to have the ability to capture the hundreds of fluorescence spectra per second required for transient bursts of high concentration aerosols. In addition, a field-portable instrument needs components that are compact and light. A multi-anode PMT assembly that has recently become available holds promise for building on these recent advances for detection of bio-aerosol particles. Replacing the cooled ICCD with a multi-anode PMT detector would increase the spectrum recording speed and reduce the physical size of the detection system.

In this article we report a high-speed, high-sensitivity aerosol fluorescence spectrum detection system that employs a new 32-anode PMT assembly (Hamamatsu, H7260) together with the interface electronics (Vtech Engineering, PhotoniQ P7260-1). By collecting the fluorescence emission

[a)]Electronic mail: richard.chang@yale.edu

from single aerosol particles excited by single laser pulses, the system is capable of detecting and recording the fluorescence spectra at repetition rate in excess of 1400 particles per second, while maintaining single-photon sensitivity. The 32-anode PMT and its electronics assembly are suitable for a real-time, field-portable detection system.

II. EXPERIMENTAL APPARATUS AND DESCRIPTION

An aerosol fluorescence spectrum analyzer that employs an ICCD detector has been described in detail previously.[4,8] Briefly, the detection system works as follows. Particles entrained within a stream of air are directed toward a trigger volume, defined by the intersection of two (635 and 670 nm wavelength) near 90° crossed diode laser beams. A trigger pulse from the AND gate is generated only when the elastic scattering of light, detected by two PMTs, exceeds a preset threshold from a single particle crossing simultaneously both of these beams. The illuminating *Q*-switched UV laser is set to fire and the ICCD to gate on about 1 μs later after the trigger pulse from the AND gate, while the particle travels the short downstream distance ($\sim$20 μm) between the trigger volume and the sample volume. The sample volume is determined by the intersection of the focal region of the illuminating laser (which excites fluorescence in the targeted particle) and the focal point of the reflective objective (which collects the fluorescence). The illuminating laser is a diode-pumped, *Q*-switched, pulsed laser of 266 nm (or 355 nm) wavelength, with 30 ns (or 70 ns) duration, operating at the fourth harmonic (or the third harmonic) of a Nd:yttrium–aluminum–garnet (YAG) laser (Spectra Physics model X-30 or Y-70). Fluorescence emitted from the particle is collected by a high numerical aperture (NA=0.5) Schwarzchild reflecting objective, and dispersed by a spectrograph (Acton SP-150, with 300 groove/mm grating blazed at 500 nm). A cooled ICCD camera is placed at the spectrograph exit plane. A long-pass filter is placed in front of the spectrograph in order to pass the fluorescence and block the elastically scattered light of the UV laser.

In our new system, we exploit a different detector and develop a data acquisition and storage capability for the detector. We refer to this advancement as a high-speed aerosol fluorescence spectrum analyzer (HAFSA). The HAFSA employs a 32-anode PMT detector having a single photocathode and nine dynode stages that preserve spatial integrity across the photocathode. Acquisition and storage of the 32 separate data channels are facilitated by interface electronics (hereafter referred to as PhotoniQ), a data acquisition board (National Instruments, BNC-2110), and software written for experimental control and acquisition in C programming language.

To describe the operation of the HAFSA, consider a time sequence of its detection and data processing system functions revealed in Fig. 1. The diagram indicates the sequence of an event cycle. Time evolution is from left to right and anode number (or wavelength) is from front to back. The AND gate trigger output starts the event cycle; subsequently the following events occur: (1) the sampling of background levels for all PMT anode channels; (2) the firing of the

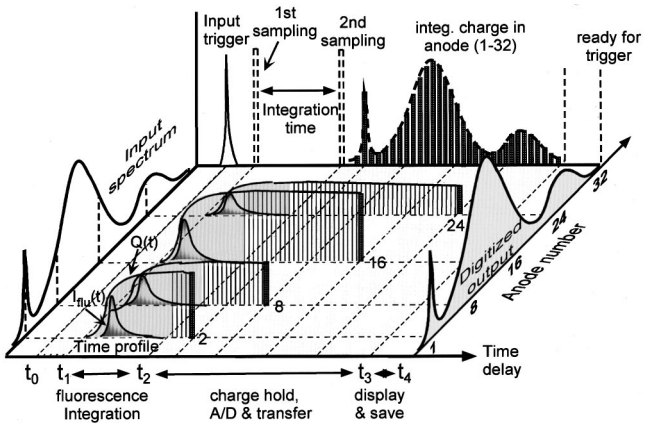

FIG. 1. A schematic diagram for the fluorescence detection and data processing. Time evolution is from left to right and anode number (or wavelength) is from front to back. One event cycle can be described as follows. An input trigger starts the event cycle. All the PMT anodes are sampled for the background, the *Q*-switched laser fires, the fluorescence emits, all anodes are integrated for their charges, analog to digital converts the sampled voltages at each of the 32 PMT anodes, data are serially transferred to a computer, the single-shot fluorescence spectrum is displayed and stored, and at last the whole system is reset and rearmed for another trigger pulse.

Q-switched laser; (3) the fluorescence emission excited by the laser; (4) the conversion of fluorescence photons to photoelectrons at the PMT photocathode; (5) the photoelectron cascade and integration of charges from each anode; (6) the analog-to-digital sampling of voltages for each of the 32 PMT channels; (7) the serial transfer of these digital voltage values to a computer port; (8) the subsequent display and storage of the single-shot fluorescence spectrum; and (9) the resetting and rearming of the system for another trigger pulse from the AND gate.

Specific timing and integration of these functions is as follows. About 1 μs after the initial trigger pulse at time t_0, a delay/pulse generator fires two independent but synchronous trigger pulses. The first pulse is fed to the PhotoniQ to start an acquisition cycle, and the second pulse to trigger the *Q*-switched pulsed laser, which illuminates the targeted aerosol particle. The PhotoniQ has a data acquisition channel for each of the 32 anodes of the PMT. Each channel contains a wideband, integrating, preamplifier, a background subtraction circuit, and a wideband 14 bit analog-to-digital converter (ADC). The ADC first samples the background at time t_1 just before the laser fires and before the preamplifiers begin to simultaneously integrate the charges from each of the 32 anodes. The time-delay t_1-t_0 is set by the pulse-delay generator (to be about 1 μs) as required by the trigger of the *Q*-switched laser. In addition to the external delay generator, the PhotoniQ interface provides a built-in digitally controlled delay generator (over a range of 80–280 ns) for fine timing control that can be set through an RS-232 port. The emitted fluorescence, after being dispersed by the spectrograph (see Fig. 2), reaches the photocathodes of the 32-anode PMT with spatially distributed, wavelength-dependent intensity. The fluorescence intensity increases with the laser pulse and decays to zero within a few nanoseconds after the laser pulse ends. The 32 charge-integrating preamplifiers in the PhotoniQ simultaneously capture the charges from the 32 anodes

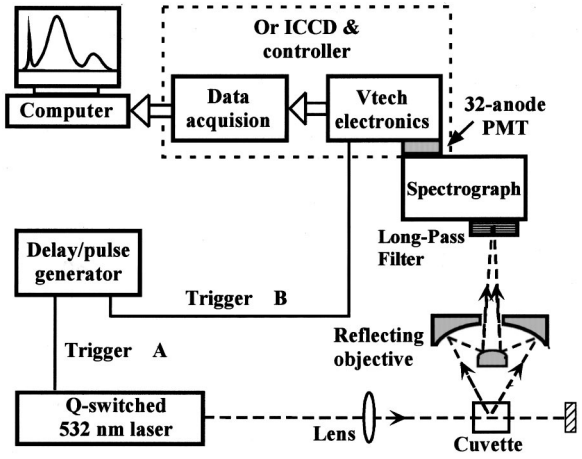

FIG. 2. A schematic setup for testing the complexity of the high-speed aerosol fluorescence spectrum analyzer (HAFSA). A cuvette containing 2×10^{-8} M rhodamine 640 dye was used instead of an aerosol source for convenience. The cuvette was illuminated by a single pulse (52 nJ) from the second harmonic (532 nm) of the Nd:YAG laser (30 ns duration). Fluorescence emitted from the dye is collected by a Schwarzchild reflecting objective [(NA=0.5), and dispersed by a spectrograph (Acton SP-150, with 300 groove/mm grating blazed at 500 nm]. The fluorescence spectrum exited from the spectrograph is detected by a 32-anode PMT or a cooled ICCD camera and their corresponding controllers. A long-pass filter is placed in front of the spectrograph in order to pass the fluorescence and block the elastically scattered light of the laser.

during the integration period from t_1 to t_2. This time period is configured through the RS-232 line to the PhotoniQ and can be adjusted between 340 and 540 ns. The ADCs capture the sample voltages from the 32 integrating preamplifiers after the integration period is complete. The net voltage is then the difference between the first sample prior to integration and the second sample following the integration. This differential approach helps minimize susceptibility to electromagnetic fields or other low frequency noise.

The output data stream (sampled voltages) from each channel is serially transmitted through a single analog line from the PhotoniQ. This stream is created by passing the converted data words through a digital-to-analog converter (DAC) prior to being buffered and transmitted differentially out the analog port. The DAC maintains the analog output of each channel for 10 μs and provides a digital readout clock that occurs 9 μs after each data transition. An entire 32-element event vector can be read out in 640 μs, corresponding to the time from t_2 to t_3. A 12 bit data acquisition card is used to recapture the data into the PC. Figure 1 shows the time profiles of fluorescence intensity $[I_{\mathrm{flu}}(t)]$ and the corresponding integrated charge $[Q(t)]$ for several channels.

Serial analog data transmission from the PhotoniQ to the data acquisition card was chosen for this application as a compromise between speed and system complexity. The PhotoniQ can also provide digital transmission of the fluorescence data directly to the PC through the serial RS-232 link with the full 14 bit data resolution without the data acquisition card, but this significantly reduces the maximum event rate.

Integral to the operation of the HAFSA is the control and acquisition software. The software for experimental control and data acquisition, data processing, spectral display, and data analysis is written in the C programming language using National Instruments Labwindows/CVI 4.01. The system is operated with a PC (Gateway 2000) by means of the RS-232 communication port. Upon command, the computer sends a signal to ask the PhotoniQ to wait for the next trigger pulse and measure the next single-shot spectrum. The whole process for taking one single-shot spectrum requires less than 700 μs. Additional triggers that arrive before the completion of the event are ignored. The fluorescence spectra data obtained through the data acquisition card or through the RS-232 port can be immediately plotted on the computer screen. The data can also be saved in the host PC for later analysis. Numerous consecutive single-shot spectra or a series of accumulated single-shot spectra can be selected for display or/and saving. The wave forms displayed on the screen can be manually or automatically rescaled. Anode location and intensity can be read from the screen via the mouse cursor, which is convenient for real-time wavelength calibration.

One of the chief advantages the HAFSA system has over a similar detection system employing an ICCD detector is the high sample rate. For higher event rates approaching 40 000 per second, the PhotoniQ design contains a high-speed batch mode. In the batch mode, the data are not transmitted out of the analog port after every event, as this limits the overall event rate. Instead, the data from each event are stored temporarily in on-board memory. After a fixed number of events have been captured (up to several thousand), the data can be accessed via the RS-232 link and read into a host PC memory for further analysis. In this way, batches of very high-speed data can be captured in real time and read into the PC at a slower rate. One advantage of this digital output mode is that the experimenter need not worry about signal corruption in the analog domain after the data has already been cleanly captured into the digital domain.

III. EXPERIMENTAL PERFORMANCE AND DISCUSSION

A. Wavelength calibration and spectral response

Wavelength calibration of the HAFSA multi-anode PMT was done using the fourth harmonic (266 nm) and second harmonic (532 nm) of the Nd:YAG laser, and the 635 nm diode laser as light sources. The current system covers the wavelength range from 205 to 835 nm with a spectral resolution of 20 nm. Thus, the HAFSA is suitable for the detection of bioaerosols having broad fluorescence emission bands.

The spectral response of the HAFSA was determined as follows. First, before the 32-anode PMT was connected to the PhotoniQ, the gain of each channel was calibrated by injecting known charges into the integrators and reading the resulting voltage levels from the PC. The average gain (scale factor) for each channel is 35.6 ± 0.5 mV/pC at the output for differential data acquisition. Next, the PMT was connected to the interface, and a 500 W quartz tungsten halogen lamp (Oriel) was used to calibrate the spectral response of the *relative intensities of the combination of* PMT *and spectrograph*. The number of photons (*absolute intensity*) reaching the PMT can be calculated by reading the output voltage

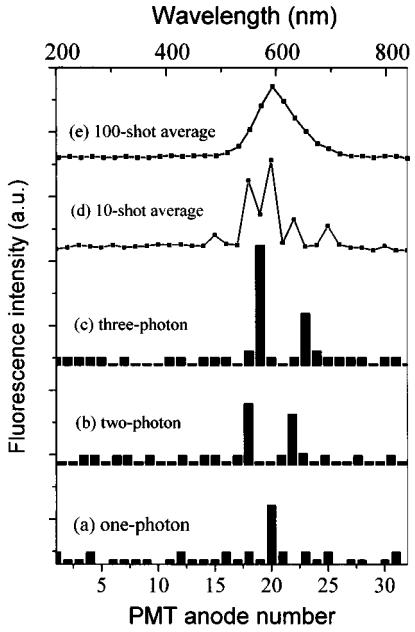

FIG. 3. Typical single-shot fluorescence spectra detected by HAFSA at an incident intensity of single photon-electron level. The conversion of photoelectrons to photons assumes the quantum efficiency to be 20%. (a) Only one photon was captured by the 20th channel of all 32 PMT anodes; (b) two photons were recorded in the 18th and 22th channels; spectrum (c) two photons were recorded in the 19th channel and another single-photon event in the 23rd channel; (d) and (e) were 10- and 100-shot average spectra reveal a fluorescence spectral profile of the R-640 dye excited by a 532 nm laser.

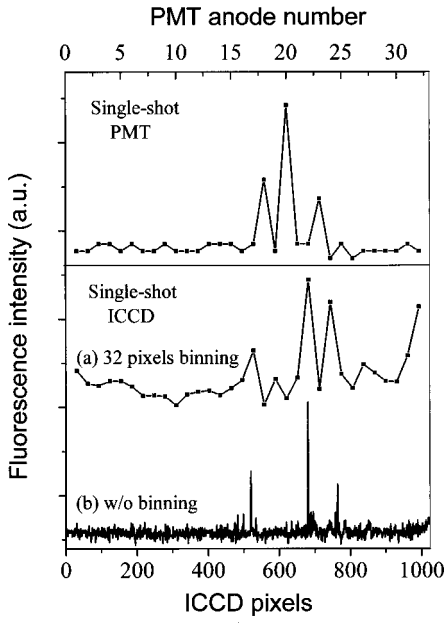

FIG. 4. Comparison of the sensitivity between the 32-anode PMT (upper part) and the cooled ICCD detector (lower part). Both systems under the same experimental conditions detected four photons in their single-shot fluorescence spectra. Both spectra display single-photon sensitivity and have comparable signal-to-noise ratios.

from the PC and using the specific quantum efficiency of the photocathode at each measured wavelength, the gain of the PMT at the applied voltage (*calibrated by Hamamatsu for this specific PMT by using a standard lamp of 2856 K*), and the scale factor between the output voltage and the charges transferred from the PMT to the PhotoniQ.

B. Sensitivity of the HAFSA

The sensitivity of the HAFSA has been tested and compared with a similar detection system employing a cooled ICCD camera (Princeton Instruments, 1024 MLDS-E). A schematic diagram of the test setup is shown in Fig. 2. For experimental convenience a cuvette containing 2×10^{-8} M rhodamine 640 (R-640) dye was used instead of an aerosol source. The cuvette was illuminated by a single pulse (52 nJ) from the second harmonic (532 nm) of the Nd:YAG laser (30 ns duration), with 850 V voltage applied to the PMT. The trigger pulses for firing the laser and activating the PhotoniQ were generated by a delay/pulse generator. Their time delay (0.64 μs) was optimized by maximizing the fluorescence signal. The laser pulse energy was then reduced using neutral density filters until the fluorescence intensity corresponded to a few photons detected with a single laser shot.

The spectra in Figs. 3(a)–3(c) are typical of single-shot results, where the number of photoelectrons are converted to photons by using the photon quantum efficiency 20%. In spectrum (a), only one photon was captured by the 20th channel of all 32 PMT anodes; in spectrum (b), two photons were recorded in the 18th and 22nd channels; while in spectrum (c), two photons were recorded in the 19th channel and another single-photon event in the 23rd channel. The accumulation results shown [10-shot average-spectra (d) and 100-shot average-spectra (e)] reveal a more familiar fluorescence spectral profile of the R-640 dye excited by a 532 nm laser.

For comparison, the ICCD camera-based system was also used to detect the same low level single-shot fluorescence. This detector was cooled to -30 °C and the gain set at 8.5 (maximum 10) for supplying high voltage to the image intensifier. Figure 4 shows a typical ICCD spectra for the same conditions. Both PMT (upper part of Fig. 4) and ICCD (lower part of Fig. 4) detection systems detected four photons in their single-shot spectra. They both have single-photon sensitivity. For comparison with the 32 anode–PMT, the single-shot spectrum detected with the ICCD [1024 pixels, see spectrum (b) in Fig. 4] was binned to 32 channels [see spectrum (a) in Fig. 4]. The spectra are comparable, and the PMT detector shows a better signal-to-noise ratio.

C. Data rate for the HAFSA

In order to determine the maximum rate at which fluorescence spectra can be measured with the HAFSA, two laser pulses were used to excite fluorescence from R-640 dye in the cuvette. The time interval between the two pulses was then decreased until the system was no longer able to record two sequential fluorescence spectra. For ICCD, the minimum time between laser pulses was found to be 40 ms, corresponding to a maximum spectra data rate of 25 Hz. By contrast, for the HAFSA, which uses the 32-anode PMT detector, the shortest time between two pulses was 700 μs, corresponding to a data rate of 1400 Hz to record fluorescence spectra.

To emphasize the utility of the fast data rate of the HAFSA, we measured the single-shot fluorescence spectra

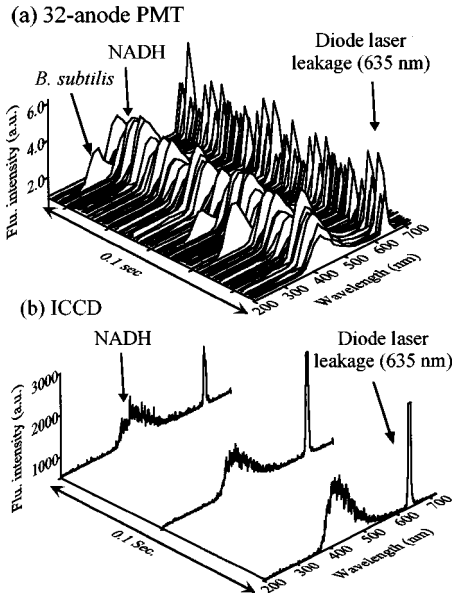

FIG. 5. Consecutive single-shot fluorescence spectra of aerosolized (≈ 5 μm in diameter) *Bacillus subtilis* bacteria and NADH mixture taken by the 32-anode PMT and ICCD-based detector systems. Within 0.1 s, the 32-anode PMT system captured 100 fluorescence spectra (can reach a repetition rate of 1.4 KHz). Because of the difference in the particle density, only 3 *Bacillus subtilis* bacteria spectra (peaked at 330 nm) were detected while dominated by the NADH aerosols (97 spectra, peaked at 450 nm). Under the same experimental conditions, the ICCD-based detector captured only 3 NADH fluorescence spectra in all. The sharp peak at 635 nm is the elastic scattering from the diode laser.

from aerosols containing a mixture of two types of particles. These aerosols are the mixing output of two ink-jet aerosol generators (IJAG), which can produce monodispersed aerosols at a rate between 1 Hz and 2 kHz with mean diameter between 1 and 10 μm in diameter (15% variation in size).[10] We chose for this test a mixture containing a high concentration of reduced nicotinamide adenine dinucletides (NADH) together with a low concentration of bacteria cells. The high concentration NADH (Sigma) was aerosolized (5 μm diameter) at 4 kHz by one IJAG, and the low concentration *Bacillus subtilis* (vegetative cells, Sigma) was aerosolized (also 5 μm diameter) at 80 Hz by a second IJAG. Thus the bacteria aerosol concentration was about 2% of the total.

Figure 5 presents the consecutive single-shot fluorescence spectra of this aerosol mixture, taken over 0.1 s, for both 32-anode PMT and ICCD-based detector systems. The HASFA fluorescence detection system with the 32-anode PMT captured 100 fluorescence spectra within 0.1 s in which 97 spectra are from the high concentration of NADH (having fluorescence band around 450 nm) and the remaining three spectra are from *Bacillus subtilis* bacteria (having a spectral band peaked at 330 nm). Under the same conditions, the ICCD-based detector captured only three fluorescence spectra, all of them corresponding to NADH. This comparison demonstrates the capability of the HASFA (with the 32-anode PMT detection) to capture the fluorescence spectra of a minority concentration of potentially harmful aerosol entrained within an innocuous concentration of background aerosol.

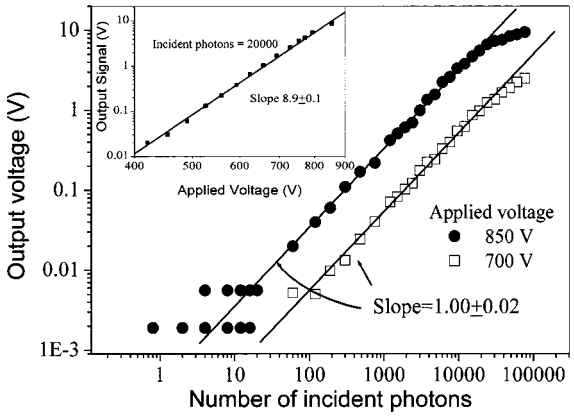

FIG. 6. A typical output voltage from one particular channel (the 20th of the 32 channels of HAFSA system) varies linearly with the input of photons (up to *20 000* photons) with the applied voltage at 700 V, and starts to saturate with the applied voltage at 850 V. The inset shows the corresponding output voltage varies superlinearly (with a slope 8.9 ± 0.1) with the applied voltage on the 32-anode PMT while keeping the incident illumination constant (at around *20 000* photons per pulse).

D. Dynamic range and linearity

The PhotoniQ provides 14 bits of resolution with a full scale differential analog output of 10 V. The rms equivalent thermal noise charge of the PhotoniQ is below the level of a single least significant bit (LSB), thereby preserving the full 84 dB dynamic range. One LSB, measured at the analog output, is 0.61 mV (corresponding to 17 fC of charge at the input). Thus, the relationship between the system LSB and the output from a single photoelectron event depends on the PMT gain, but for reasonable gain settings the PhotoniQ dynamic range will include single photoelectron events.

Figure 6 shows a typical linearity measurement from one (the 20th) of the 32 channels with a 700 and 850 V applied voltage for the 32-anode PMT. The system has a 1.9 ± 0.4 mV output offset when the PMT is in the dark. A single photoelectron event appears around 7.5 mV (5.6 mV once the offset is subtracted), with the repetition of 7.5 mV for the next few points in Fig. 6 demonstrating the statistical nature of the PMT's 5% quantum efficiency *at 585 nm (on average 20 photons produce 1 photoelectron)*. When the PMT is applied with 700 V, the output increases linearly with the incident fluorescence up to *80 000 photons (within 30 ns, corresponding to 4000 photoelectrons)* in our measurement range. While it is applied with 850 V, the output linearly rises with increased incident fluorescence until 8 V, when the illuminating fluorescence reaches about *20 000* photons. The output deviation starting at 8 V could be attributable to several sources, i.e., either the PMT or the PhotoniQ electronics. For the PMT, both cathode and anode will cause *deviation from linearity* at large currents. *The linear range varies with different wavelength and, hence, the deviation point is dependent on the wavelength through the quantum efficiency*. Examining the possibility of cathode saturation, the cathode saturation current for a PMT is from 0.1 to 10 μA according to different cathode materials.[11] Therefore, the number of incident photons required to saturate the cathode using a 30 ns light pulse (consider the time profile of the fluorescence to

be essentially the same as that of the laser pulse) can be estimated as

$$i\Delta(t)/e\eta = (0.1\times 10^{-6}) \times (30\times 10^{-9})/[(1.6\times 10^{-19})\times(5\%)] = 37.6\times 10^{4} \text{ (photons)}.$$

This value is much higher than the measured level at which the output nonlinearity occurred, so the observed saturation is most likely not caused by the PMT cathode. The linearity at lower applied voltage also proves that the saturation is not caused by the photocathode. The space charge will dominate the anode linearity when the PMT is used in pulsed applications. A PMT anode will generally saturate when the last dynode current reaches around 10 mA.[11] For the 30 ns laser pulse, this current level corresponds to an output of 10.8 V it is 25% above the observed level. Considering that the minimum anode saturation current is not a manufacturer-specified parameter, and the peak current generated by the laser pulse is larger than 10 mA, the average calculated value, it is reasonable to speculate that this PMT unit may begin to be saturated around 8 V.

The output voltage of the whole system at different PMT applied voltages (from 400 to 900 V) was also measured (see the inset of Fig. 6) in order to compare the gain of the PMT, the detector itself to the gain of the whole system. The output voltage was shown to correlate very well with the expected PMT dependence on the applied voltage. This is described by

$$V_{\text{output}} = A\times (V_{\text{applied}})^{kn}.$$

For a PMT, A, and k are constants determined by the PMT structure and material of the dynode, with k generally ranging from 0.7 to 0.8 and n is the number of dynode stages. The measured kn of the whole system was 8.9 ± 0.1, very close to the PMT kn value of 8.6 ± 0.3. Thus, the whole system preserves the gain of the PMT itself without significant distortion.

E. Noise, crosstalk, and stability

The noise observed at the system output, which was measured to be 0.43 mV rms, is a combination of PMT noise and interface electronics noise. This noise level is not only less than the charge resulting from a single incident photoelectron, it is below the level of a single 14 bit LSB. When the PMT is applied with 800 V the signal from a single photoelectron is 4.3 times greater than the peak amplitude of the thermal noise (using $3\sigma = 1.3$ mV as the highest peak noise level) and is therefore easily picked out from the noise.

Two sources of crosstalk are relevant in the system. The first is within the 32-anode PMT, especially between physically adjacent channels. Hamamatsu specifies the crosstalk between adjacent channels within the PMT to be typically 3%. The second source is the PhotoniQ. The average crosstalk between adjacent PhotoniQ channels was measured to be 0.06%, with a maximum value of 0.10%. Thus, the PhotoniQ will contribute little crosstalk to the fluorescence spectrum as compared to the PMT itself.

Stability, or output variation with time, is also important for obtaining accurate data. Instability is generally due to a decrease in the secondary emission ratio over long periods of operation, short time drift, and hysteresis phenomena in PMTs. It is reported that the long-term instability of the PMT is within 1%–2% over several tens of hours.[11] The short-term drift and hysteresis phenomena can be reduced by system warmup, using stabilized power supply, pre-operation with a dummy light source, and well-grounded wiring with electromagnetic protection. When recording fluorescence spectra, variations in spatial uniformity between different channels are much more serious than the several percent variation in the overall system gain, which just affects the absolute intensity of the whole spectrum without changing the spectral profile. The double sampling done by the PhotoniQ greatly reduces the base drift of the system, and most low frequency variation in the optical background.

ACKNOWLEDGMENTS

New Mexico State University acknowledges financial support from the U.S. Army Research Laboratory (ARL, DAAL01-98-C0056). Yale University acknowledges the partial financial support from the U.S. Army Research Office (DAAG55-97-1-0349), the Air Force Research Laboratory, and ARL (DAAL01-97-2-0128), and an Augmentation Award for Science and Engineering Research Training (AASERT) Fellowship (DAAG-97-1-0199) for S. Holler.

[1] R. G. Pinnick, S. C. Hill, P. Nachman, J. D. Pendleton, G. L. Fernandez, M. W. Mayo, and J. G. Bruno, Aerosol. Sci. Technol. **23**, 653 (1995).
[2] G. Chen, P. Nachman, R. G. Pinnick, S. C. Hill, and R. K. Chang, Opt. Lett. **21**, 1307 (1996).
[3] P. P. Hairston, J. Ho, and F. R. Quant, J. Aerosol. Sci. **28**, 471 (1997).
[4] Y. L. Pan, S. Holler, R. K. Chang, S. C. Hill, R. G. Pinnick, S. Niles, and J. R. Bottiger, Opt. Lett. **24**, 116 (1999).
[5] Y. S. Cheng, E. B. Barr, B. J. Fan, P. J. Hargis, Jr., D. J. Rader, T. J. OíHern, J. R. Torczynski, G. C. Tisone, B. L. Preppernau, S. A. Young, and R. J. Radloff, Aerosol. Sci. Technol. **30**, 186 (1999).
[6] J. D. Eversole, J. J. Hardgrove, W. K. Cary, Jr., D. P. Choulas, and M. Seaver, Field Anal. Chem. Technol. **3**, 249 (1999).
[7] F. L. Reyes, T. H. Jeys, N. R. Newbury, C. A. Primmerman, G. S. Rowe, and A. Sanchez, Field Anal. Chem. Technol. **3**, 240 (1999).
[8] S. C. Hill, R. G. Pinnick, S. Niles, Y. L. Pan, S. Holler, R. K. Chang, J. R. Bottiger, B. T. Chen, C. S. Orr, and G. Feather, Field Anal. Chem. Technol. **3**, 221 (1999).
[9] P. H. Kaye, J. E. Barton, E. Hirst, and J. M. Clark, Appl. Opt. **39**, 3738 (2000); K. L. Schroder, P. J. Hargis, R. L. Schmitt, D. J. Rader, and I. R. Shokair, Proc. SPIE **3833**, 82 (1999).
[10] J. R. Bottiger, P. J. Deluca, E. W. Stuebing, and D. R. Vanreenen, J. Aerosol Sci. Suppl. **29**, S965 (1998).
[11] Hamamatsu Photonics K. K editorial committee, *Photomultiplier Tube Principle to Application* (Hamamatsu Photonics K. K, Japan, 1994).